Adaptive Generative Models for Digital Wireless Channels

Omar S. Salih, *Member, IEEE*, Cheng-Xiang Wang, *Senior Member, IEEE*,
Bo Ai, *Senior Member, IEEE*, and Raed Mesleh, *Senior Member, IEEE*

***Abstract*—Generative models, which can generate bursty error sequences with similar burst error statistics to those of descriptive models, have an immense impact on the wireless communications industry as they can significantly reduce the computational time of simulating wireless communication links. Adaptive generative models aim to produce any error sequences with any given signal-to-noise ratios (SNRs) by using only two reference error sequences obtained from a reference transmission system with two different SNRs. Compared with traditional generative models, this adaptive technique can further considerably reduce the computational load of generating new error sequences as there is no need to simulate the whole reference transmission system again. In this paper, reference error sequences are provided by computer simulations of a long term evolution (LTE) system. Adaptive generative models are developed from three widely used generative models, namely, the simplified Fritchman model (SFM), the Baum-Welch based hidden Markov model (BWHMM), and the deterministic process based generative model (DPBGM). It is demonstrated that the adaptive DPBGM can provide accurate burst error statistics and bit error rate (BER) performance of the LTE system, while the adaptive SFM and adaptive BWHMM fail to do so.**

***Index Terms*—Adaptive generative models, error models, burst error statistics, Markov models, hidden Markov models.**

Manuscript received September 3, 2013; revised January 31, 2014; accepted May 1, 2014. Date of publication May 16, 2014; date of current version September 8, 2014. This work was supported in part by the EPSRC and Philips Research Cambridge, U.K.; by the Opening Project of the Key Laboratory of Cognitive Radio and Information Processing, Guilin University of Electronic Technology, Ministry of Education under Grant 2013KF01; by the State Key Laboratory of Rail Traffic Control and Safety, Beijing Jiaotong University under Grant RCS2012K003; by National 863 project in 5G, Ministry of Science and Technology, China under Grant 2014AA01A706; by the National Natural Science Foundation of China under Grant 61222105; by the Beijing Municipal Natural Science Foundation under Grant 4112048; by the Sensor Networks and Cellular Systems Research Center, University of Tabuk; and by the Ministry of Higher Education in Saudi Arabia. The associate editor coordinating the review of this paper and approving it for publication was A. Zajic.

O. S. Salih is with the Department of Aerospace, Electrical and Electronic Engineering, Faculty of Engineering and Computing, Coventry University, Coventry CV1 5FB, U.K. (e-mail: omar.salih@coventry.ac.uk).

C.-X. Wang is with the School of Information Science and Engineering, Shandong University, Jinan 250100, China, the Institute of Sensors, Signals and Systems, School of Engineering and Physical Sciences, Heriot-Watt University, Edinburgh EH14 4AS, U.K., and also with the Sensor Networks and Cellular Systems Research Center, University of Tabuk, Tabuk 71491, Saudi Arabia (e-mail: cheng-xiang.wang@hw.ac.uk).

B. Ai is with the State Key Laboratory of Rail Traffic Control and Safety, Beijing Jiaotong University, Beijing 100044, China (e-mail: aibo@ieee.org).

R. Mesleh is with the Sensor Networks and Cellular Systems Research Center, University of Tabuk, Tabuk 71491, Saudi Arabia (e-mail: rmesleh.sncs@ut.edu.sa).

Color versions of one or more of the figures in this paper are available online at http://ieeexplore.ieee.org.

Digital Object Identifier 10.1109/TWC.2014.2325028

I. Introduction

A DIGITAL (time-discrete) channel generally represents the whole wireless communication chain, including the transmitter, analog (or physical) channel, and receiver in the complex baseband. The input and output of a digital channel are in the digitized form. Because of impairments in wireless channels, errors frequently emerge in digital channels. Moreover, signal processing in many components of the wireless transmission system may add further errors [1]. It is perceived that these errors arising from digital wireless channels with memory are not independent but appear in clusters or bursts. Bursty error sequences can be statistically represented by mathematical channel models called error models [2], which can be classified as descriptive [3] and generative [4] models. Descriptive models express the burst error statistics of reference error sequences obtained directly from experiments. Generative models have mechanisms that can generate error sequences having any required length and burst error statistics similar to those of reference error sequences. Compared with descriptive models, generative models are more efficient as they do not need to simulate the whole communication system and therefore can significantly reduce the simulation time of generating error sequences. The main applications of error models are to assist in the performance assessment and design of error control schemes and high layer wireless communication protocols [5]–[9]. Error models can characterize error sequences in either bit level or packet level [10], [11].

In the literature, there are five main classes of generative models. Markov models are the first class of generative models consisting of finite [12]–[17] or infinite states [4] in a chain. The Gilbert-Elliot model [12], [13] was the first finite-state Markov model with only two states for generating errors and error-free bits. It produces error sequences with burst error statistics that diverge significantly from the desirable ones. An increase in the number of states can achieve better performance [11], [14], [15]. For example, simplified Fritchman's models (SFMs) [14], [18], [19] replaced the error-free state of the two-state Markov model with a group of error-free states while keeping the only error state. Bipartite models [11] are more advanced Markov models, but their complexity is very high in order to achieve a satisfactory accuracy of burst error statistics. The second class is hidden Markov models (HMMs) [20]–[23], which contain hidden parameters that can be calibrated through observations. The Baum-Welch (BW) algorithm [24] was mostly used to attune the hidden parameters based on available observations, resulting in the so-called BW based HMMs (BWHMMs).

Compared with finite-state Markov models, HMMs are much more complicated due to the huge number of states required to train the hidden parameters, which greatly increases the computational speed. The third and fourth classes of generative models are based on stochastic context-free grammars (SCFGs) [25] and chaos theory [26]–[29], respectively. SCFGs consist of production rules and symbols, each of which is assigned a probability that controls its behavior. These models are limited to error bursts with bell-shaped error density distributions. Chaotic generative models cannot describe the desired error correlation function with high accuracy [26]. The final class of generative models is the deterministic process based generative models (DPBGMs) [30]–[32], which utilize the second order statistics of fading processes. DPBGMs have proven their superiority over other generative models, e.g., SFM [31] and BWHMM [32].

All the aforementioned traditional generative models [12]–[31] were developed for error sequences corresponding to one digital channel with fixed system parameters and channel conditions, e.g., signal-to-noise ratios (SNRs). If SNRs change, the whole communication system will have to be simulated again in order to generate new reference error sequences. Consequently, those traditional generative models will have to be developed again with modified model parameters in order to fit the burst error statistics to those of new reference error sequences. However, for appropriate design and performance evaluation of error control schemes and high layer protocols, we need to test transmission schemes with many different channel conditions or SNRs. In this case, using traditional generative models are still very time consuming, as numerous reference error sequences corresponding to different SNRs have to be first produced by the reference communication system. Therefore, it is highly desirable to develop adaptive generative models that can utilize the limited (e.g., only 2) available error sequences to attain new error sequences with any SNRs without sacrificing much of the accuracy in terms of burst error statistics. To the best of our knowledge, this has never been done before.

In this paper, we propose three adaptive generative models based on well-known traditional generative models, i.e., SFM, BWHMM, and DPBGM, by adjusting some useful model parameters. Reference error sequences (descriptive models) were obtained from uncoded long term evolution (LTE) systems. The burst error statistics of newly generated error sequences using the three adaptive generative models are compared with those of reference error sequences. Also, the bit error rates (BERs) of coded LTE systems are compared using reference error sequences and new error sequences obtained from the three adaptive generative models. It is shown that the proposed adaptive DPBGM can provide excellent approximation to the desired burst error statistics of reference error sequences and the desired BER of coded LTE systems. However, the adaptive SFM and the adaptive BWHMM fail to do so.

This paper is organized as follows. Section II defines some terms related to binary error sequences and describes some important burst error statistics as performance metrics. The novel adaptive procedures for three widely used generative models, namely SFM, BWHMM, and DPBGM, are proposed in Section III. Section IV illustrates an LTE simulator which is used as a descriptive model to derive reference bit error sequences at certain values of SNR. The burst error statistics are also compared between different adaptive generative models and descriptive models in this section. Finally, conclusions are drawn in Section V.

II. Burst Error Statistics

An error sequence of a digital wireless channel can be obtained by comparing the output sequence with the input sequence. Here, we consider a binary bit error sequence as a sequence of “0”s and “1”s, which denote correctly received bit and error bit, respectively.

We can breakdown an error sequence into smaller parts in order to study its nature and calculate the burst error statistics. Therefore, a number of terms can be defined as follows. A *gap* is defined as a sequence of consecutive zeros between two ones, having a length equal to the number of zeros [18], [33]. An *error cluster* is a series of errors that occur consecutively. It has a length equal to the number of ones [14]. An *error-free burst* is defined as an all-zero sequence with a length of at least η bits, where η is a positive integer [11], [21]. Compared to a gap, an error-free burst has the minimum length of η and is not necessarily located between two errors. An *error burst* is a series of ones and zeros restricted by “1”s at the edges, and separated from neighboring error bursts by error-free bursts [11], [21]. Clearly, the minimum length of an error burst is one, and the number of consecutive error-free bits within an error burst is less than η. Hence, the local error density inside an error burst is greater than $1/\eta$.

In what follows, we list widely used burst error statistics available in the literature for characterizing bit error sequences:

1) $G(m_g)$: the gap distribution (GD), which is defined as the cumulative distribution function (CDF) of gap lengths m_g. This statistic gives some indication of the randomness of the channel [33].
2) $P(0^{m_0}|1)$: the error-free run distribution (EFRD), which is the probability that an error bit is followed by at least m_0 error-free bits [14]. The EFRD can be calculated from the GD [33]. Clearly, $P(0^{m_0}|1)$ is a monotonically decreasing function of m_0 such that $P(0^0|1) = 1$ and $P(0^{m_0}|1) \to 0$ as $m_0 \to \infty$. This statistic is very useful to determine the minimum error-free burst length η.
3) $P(1^{m_c}|0)$: the error cluster distribution (ECD), which is the probability that a correct bit is followed by m_c or more successive bits in error [14]. This statistic distinguishes between the bursty channels and random channels as well, i.e., bursty channels have long error clusters (e.g., 15–20), whereas random channels have short error clusters (e.g., 1–3).
4) $P_{EB}(m_e)$: the error burst distribution (EBD), which is the CDF of error burst lengths m_e. This statistic helps in designing the error bursts’ correcting codes [33].
5) $P_{EFB}(m_{\bar{e}})$: the error-free burst distribution (EFBD), which is the CDF of error-free burst lengths $m_{\bar{e}}$. This statistic, together with the error burst distribution,

provides the basis for determining the optimum degree of interleaving with respect to a specific code [33].

6) $P(m, n)$: the block error probability distribution (BEPD), which is the probability that at least m out of n bit are in error. This statistic is important for determining the performance of Hybrid Automatic Repeat Request (HARQ) protocols [18].
7) $\rho(\Delta k)$: the bit error correlation function (BECF), which is the conditional probability that the Δkth bit following a bit in error is also in error. The BECF is also important because it represents the burstiness of the channel [3], [4].

Burst error statistics are useful statistical means to demonstrate the structural behavior of error sequences obtained from wireless channels with memory. Consequently, they could help in the design and evaluation of error control schemes and higher layer protocols, particularly those very important burst error statistics, such as $P(m, n)$ and $\rho(\Delta k)$. Furthermore, burst error statistics are metrics to judge the relative merits of different generative models by comparing them with the descriptive model. We will use some of these statistics in Section III to develop new adaptive generative models, and we will illustrate all of them in Section IV in order to validate the proposed adaptive generative models.

III. Adaptive Generative Models

In the following subsections, we propose three adaptive generative models for producing new error sequences with any SNRs from two reference error sequences. The adopted generative models, namely, SFM, HMM, and DPBGM, are widely known in the literature and have been applied to many wireless systems. The key idea behind an adaptive generative model is to identify a fundamental feature that is used to configure the corresponding generative model and the trend of the identified feature with different SNRs. Once the trend of the fundamental feature of the generative model is found, we can parameterize the adaptive generative model to generate error sequences at any required SNRs without the need of new reference error sequences.

A. Adaptive SFM (ASFM)

A SFM consists of N-states: one error state and $N-1$ error-free states. When a SFM transits into the error state, it generates a "1" (error bit). When a transition to an error-free state occurs, the SFM generates a "0" (correct bit). While the SFM is circulating within an error-free state, "0"s are generated until a transition to the error state occurs. In this case, the SFM generates "1"s again. Transitions between the error-free states in a SFM are forbidden. The reason for having many states generating "0"s is to generate different lengths of gaps. All the transitions take place according to assigned probabilities. The probability transition matrix $\mathbf{T}$ for an N-state SFM is [14]

$$\mathbf{T} = \begin{pmatrix} P_{11} & 0 & 0 & 0 & P_{1N} \\ 0 & P_{22} & 0 & 0 & P_{2N} \\ 0 & 0 & \ddots & 0 & \vdots \\ 0 & 0 & 0 & P_{N-1N-1} & P_{N-1N} \\ P_{N1} & P_{N2} & \cdots & P_{NN-1} & P_{NN} \end{pmatrix} \tag{1}$$

where P_{ij} is the probability of transition from State i to State j $(i, j = 1, \ldots, N)$. Note that States $1, \ldots, N-1$ are error-free states, whereas State N is the error state. The transitions between the error-free states are not allowed, i.e., $P_{ij} = 0$ for $i \neq j$ and $i, j < N$. The elements of $\mathbf{T}$ can be determined from the EFRD $P(0^{m_0}|1)$ of the reference error sequence according to [14]

$$P(0^{m_0}|1) = \sum_{i=1}^{N-1} \frac{P_{Ni}}{P_{ii}} P_{ii}^{m_0}, \qquad m_0 > 0. \tag{2}$$

The EFRD can also be approximated by the weighted sum of $N-1$ exponentials given by [14]

$$P(0^{m_0}|1) \approx \sum_{i=1}^{N-1} A_i e^{a_i m_0}. \tag{3}$$

The parameters A_i and a_i can be found by using an optimization method or a curve fitting technique to match (3) with the EFRD obtained from the reference error sequence. Consequently, the elements of $\mathbf{T}$ in (1) are obtained as follows [14]:

$$P_{ii} = e^{a_i}, \quad i = 1, \ldots, N-1 \tag{4}$$

$$P_{Ni} = A_i \times P_{ii}, \quad i = 1, \ldots, N-1 \tag{5}$$

$$P_{iN} = 1 - P_{ii}, \quad i = 1, \ldots, N-1 \tag{6}$$

$$P_{NN} = 1 - \sum_{i=1}^{N-1} P_{Ni}. \tag{7}$$

Once the above transition probabilities, i.e., all the elements of $\mathbf{T}$, are known, an error sequence with any desirable length can be generated. Therefore, the key to generate a new error sequence with the required SNR from two reference error sequences for the ASFM is to obtain the EFRD of the new error sequence, as can be seen from (1)–(7).

Let us suppose that we have two reference error sequences, e.g., X and Y, with two different SNRs in dB, e.g., SNR_X and SNR_Y, respectively. Without loss of generality, we can assume that $\text{SNR}_Y > \text{SNR}_X$. Their EFRDs are denoted as $P_X(0^{m_0}|1)$ and $P_Y(0^{m_0}|1)$. The task now is to obtain the EFRD $P_Z(0^{m_0}|1)$ for a new error sequence Z with a new SNR in dB, SNR_Z.

Fig. 1 shows the EFRDs of some reference error sequences with SNRs $= 1, \ldots, 5$ dB. We can see that in the logarithmic scale, the EFRD $P(0^{m_0}|1)$ almost linearly increases with the increase of the SNR in dB at any given gap length m_0, i.e.,

$$\frac{\text{SNR}_Y - \text{SNR}_Z}{\text{SNR}_Y - \text{SNR}_X} = \frac{\log_{10}\left[P_Y(0^{m_0}|1)\right] - \log_{10}\left[P_Z(0^{m_0}|1)\right]}{\log_{10}\left[P_Y(0^{m_0}|1)\right] - \log_{10}\left[P_X(0^{m_0}|1)\right]}. \tag{8}$$

After some simple manipulations, we can rewrite (8) as

$$\log_{10}\left(P_Z(0^{m_0}|1)\right) = \alpha \cdot \log_{10}\left[P_X(0^{m_0}|1)\right] + \beta \cdot \log_{10}\left[P_Y(0^{m_0}|1)\right] \tag{9}$$

or

$$P_Z(0^{m_0}|1) = \left[P_X(0^{m_0}|1)\right]^{\alpha} \times \left[P_Y(0^{m_0}|1)\right]^{\beta} \tag{10}$$

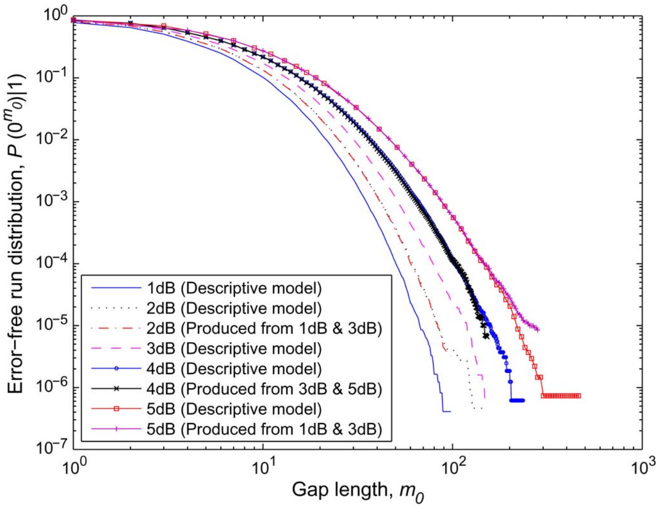

Fig. 1. The EFRDs of the descriptive model for several SNRs and reproduced EFRDs.

where α and β are defined as

$$\alpha = \frac{\mathrm{SNR}_Y - \mathrm{SNR}_Z}{\mathrm{SNR}_Y - \mathrm{SNR}_X} \tag{11}$$

$$\beta = 1 - \alpha. \tag{12}$$

Note that $\alpha < 0$ if $\mathrm{SNR}_Z > \mathrm{SNR}_Y$. Otherwise, $\alpha > 0$ holds. It is clear that α and β are simply weighting parameters to indicate the linear relationship among $\log_{10}[P_X(0^{m_0}|1)]$, $\log_{10}[P_Y(0^{m_0}|1)]$, and $\log_{10}[P_Z(0^{m_0}|1)]$. They also imply the quantity of the characteristics that the new error sequence Z inherits from reference error sequences X and Y.

Fig. 1 also shows the EFRDs of the three newly generated error sequences with SNRs $= 2$ dB (using error sequences with SNR $= 3$ dB and 5 dB, i.e., $\mathrm{SNR}_Z < \mathrm{SNR}_X$), 4 dB (using error sequences with SNR $= 3$ dB and 5 dB, i.e., $\mathrm{SNR}_X < \mathrm{SNR}_Z < \mathrm{SNR}_Y$), and 5 dB (using error sequences with SNR $=$ 1 dB and 3 dB, i.e., $\mathrm{SNR}_Z > \mathrm{SNR}_Y$), according to (10)–(12). It is clear that the EFRDs of reproduced error sequences can match those of reference error sequences with the same SNR very well, which verifies the proposed adaptive technique, as shown in (8)–(12).

B. Adaptive Baum-Welch Based HMM (ABWHMM)

HMMs [21], [23] employ the idea of Markov models, but use two stochastic processes. One stochastic process is not observable but can only be estimated by the other stochastic process which produces a sequence of observations. In [21], HMMs were implemented using BW algorithm [20], [24] and the procedure is briefly explained as follows. The error bursts of the reference error sequence are extracted and numbered. Each error burst is then divided into blocks of L bits. Each block is then represented by the number of error bits it contains. For example, when $L = 4$, the error burst 110011110001 has 3 blocks. Hence, that error burst is represented by 3 digits as 2 4 1. In this way, the error bursts are converted into a compact format as vectors, $\mathbf{NEL}_h$ ($h = 1, \ldots, \mathcal{N}_{EB}$, where $\mathcal{N}_{EB}$ is the total number of error bursts). The largest number in each $\mathbf{NEL}_h$ vector is called the peak number of errors (PNE). Therefore, we have h numbers of PNE. In the above example, PNE $= 4$ holds.

The next step is to classify the error bursts into $\mathbb{N}$ disjoint classes (submodels or bursty states) according to

$$\xi(\mathbb{N} - 1) + 1 \leq \mathrm{PNE} \leq \xi\mathbb{N} \tag{13}$$

where ξ is a positive integer. Afterwards, the compact blocks of each state shall be used to train hidden Markov submodels using BW algorithm [24]. Each submodel contains one class of error bursts. BWHMMs have the following parameters:

1) $\mathbf{S} = \{s_1, s_2, \ldots, s_{\mathbb{N}}\}$: the set of states of the model, where $\mathbb{N}$ is the number of states in the HMM.
2) $\mathbf{V} = \{v_1, v_2, \ldots, v_{\mathbb{D}}\}$: the set of observable values, where $\mathbb{D}$ is the cardinality of the observable values.
3) $\mathbf{A} = [a_{fl}]$: the state transition probabilities matrix, where a_{fl} is the probability of transition from State s_f to State s_l.
4) $\mathbf{B} = [b_{lk}]$: the observation probability matrix, where b_{lk} is the probability of emitting v_k from State s_l.
5) $\mathbf{\Pi} = [\pi_f]$: the initial state probability.

To build the BWHMM submodels, the parameters $\mathbb{N}$, $\mathbb{D}$, and the set $\lambda = \{\mathbf{A}, \mathbf{B}, \mathbf{\Pi}\}$ must be specified. The value of $\mathbb{N}$ can be decided according to the guidelines in [21]. Given a set of observation sequences (error burst blocks) representing the compact error burst $\mathbf{O}^k = \{O_1^k, O_2^k, \ldots, O_{\mathbb{D}_k}^k\}$, $k = 1, \ldots, K$ (K is the number of error bursts in each class), the BW algorithm is utilized to maximize the probability $\Gamma = \prod_{k=1}^{K} P(\lambda|\mathbf{O}^k)$ [21]. In our previous example, $\mathbf{O} = \{2, 4, 1\}$.

Once the optimized transition probabilities are found, error bursts can be generated from the submodels. To complete the generation of new error sequences, the error-free bursts concatenation to the hidden Markov submodels should be executed. The error-free bursts are represented by one state only. The transitions from the error-free state to the other states generate error bursts with variable structures according to the submodel. However, the transitions from the error burst states to the error-free state generate error-free bursts with different lengths. Both error-free bursts and error bursts are combined in the end, such that an error-free burst is followed by an error burst.

In order to generate new error sequences with any desirable SNRs from two reference error sequences, we should find out the most important feature of the BWHMM. In fact, error models aim to identify the errors and their distribution in the error bursts, and this is recognized by the $\mathbf{NEL}_h$ vector. From $\mathbf{NEL}_h$, we can know the number of errors in each block for each error burst. Consequently, from two set of vectors $\mathbf{NEL}_{hX}$ and $\mathbf{NEL}_{hY}$ corresponding to two reference error sequences X and Y with SNRs in dB as SNR_X and SNR_Y, respectively, we can obtain $\mathbf{NEL}_{hZ}$ corresponding to the new error sequence Z with SNR_Z.

Once $\mathbf{NEL}_{hZ}$ is calculated, the set of steps described before to construct the submodels are applicable in the process towards generating the required error sequence. The new error sequence Z can then be generated directly using $\mathbf{NEL}_{hZ}$ without the need for a reference error sequence. Therefore, the key to generate new error sequences with any required SNRs from two reference error sequences using the ABWHMM is to obtain the $\mathbf{NEL}_{hZ}$s of new error sequences.

In order to find $\mathbf{NEL}_{hZ}$, we need to first sort each $\mathbf{NEL}_{hX}$ and $\mathbf{NEL}_{hY}$ in a descending order so that the PNE is the leading element in each vector. Secondly, $\mathbf{NEL}_{hX}$ and $\mathbf{NEL}_{hY}$ each should be sorted in the vertical direction with a descending manner according to the values of PNE, e.g., the PNE for NEL_{1X} is greater than the PNE for NEL_{2X}. From our investigations, we have found that there also exists a linear relationship among $\mathbf{NEL}_{hX}$, $\mathbf{NEL}_{hY}$, and $\mathbf{NEL}_{hZ}$ with the decrease of SNRs in dB. Similar to the derivations in (8)–(12), we can obtain $\mathbf{NEL}_{hZ}$ from

$$\mathbf{NEL}_{hZ} = \lfloor \alpha \cdot \mathbf{NEL}_{hX} + \beta \cdot \mathbf{NEL}_{hY} \rfloor. \quad (14)$$

Here, $\lfloor \cdot \rfloor$ denotes the floor function, α and β are given by (11) and (12), respectively. Afterwards, we apply the classification rule and training procedure to generate new error bursts.

To generate error-free bursts related to the new error sequence Z, we interpolate two error-free burst distributions related to error sequences X and Y. Moreover, the number of error-free bursts of Z is obtained by interpolation from the numbers of error-free bursts of X and Y. Subsequently, the error-free burst lengths are worked out and substituted with zeros. Eventually, concatenation of new error bursts and error-free bursts is performed to produce the error sequence Z.

C. Adaptive DPBGM (ADPBGM)

The idea of the DPBGM is derived from second-order statistics of fading processes [31]. As a matter of fact, some statistics of bursty errors are related to second-order statistics of fading envelope processes. Accordingly, fading processes can be used to generate error sequences where fading intervals and inter-fading intervals are associated with error bursts and error-free bursts, respectively.

The error burst lengths and error-free burst lengths of a reference error sequence can be recorded as vectors called $\mathbf{EB}_{rec}$ and $\mathbf{EFB}_{rec}$, respectively. Let us denote the minimum value in $\mathbf{EB}_{rec}$ as m_{B1} and the maximum value as m_{B2}. Subsequently, the lengths m_e of error bursts satisfy $m_{B1} \leq m_e \leq m_{B2}$. By analogy, the minimum value and the maximum value in $\mathbf{EFB}_{rec}$ are denoted as $m_{\bar{B}1}$ and $m_{\bar{B}2}$, respectively; and the lengths $m_{\bar{e}}$ of error-free bursts satisfy $m_{\bar{B}1} \leq m_{\bar{e}} \leq m_{\bar{B}1}$. In order to proceed with the ADPBGMs design, some quantities need to be defined.

1) N_t is the total length of the reference error sequence.
2) $\mathcal{N}_{EB}$ is the total number of error bursts, which is equal to the number of entries in $\mathbf{EB}_{rec}$.
3) $\mathcal{N}_{EFB}$ is the total number of error-free bursts, which is equal to the number of entries in $\mathbf{EFB}_{rec}$.
4) $N_{EB}(m_e)$ is the number of error bursts of length m_e in $\mathbf{EB}_{rec}$. Thus, $\sum_{m_e=m_{B1}}^{m_{B2}} N_{EB}(m_e) = \mathcal{N}_{EB}$ holds. Then, the EBD $P_{EB}(m_e)$ can be calculated by $P_{EB}(m_e) = (1/\mathcal{N}_{EB}) \sum_{x=m_{B1}}^{m_e} N_{EB}(x)$.
5) $N_{EFB}(m_{\bar{e}})$ is the number of error-free bursts of length $m_{\bar{e}}$ in $\mathbf{EFB}_{rec}$. Similarly, $\sum_{m_{\bar{e}}=m_{\bar{B}1}}^{m_{\bar{B}2}} N_{EFB}(m_{\bar{e}}) = \mathcal{N}_{EFB}$ holds. Then, the EFBD $P_{EFB}(m_{\bar{e}})$ is given by $P_{EFB}(m_{\bar{e}}) = (1/\mathcal{N}_{EFB}) \sum_{x=m_{\bar{B}1}}^{m_{\bar{e}}} N_{EFB}(x)$.

The DPBGM consists of a sampled deterministic process followed by a threshold detector and two parallel mappers. The complex fading deterministic process can easily be approximated and represented by [31], [34]–[37]

$$\tilde{\zeta}(t) = |\tilde{\mu}_1(t) + j\tilde{\mu}_2(t)| \quad (15)$$

where

$$\tilde{\mu}_i(t) = \sum_{n=1}^{N_i} c_{i,n} \cos(2\pi f_{i,n} t + \theta_{i,n}), \quad i = 1, 2. \quad (16)$$

Here, N_i is the number of sinusoids, $c_{i,n}$ are gains, $\theta_{i,n}$ are phases from the realizations of the random generators, and $f_{i,n}$ are the discrete frequencies. To complete the parametrization of the deterministic fading process, the vector $\mathbf{\Psi} = (N_1, N_2, r_{th}, \sigma_0, f_{\max}, T_A)$ is required, where r_{th} is the envelope threshold, σ_0 is the square root of the mean power of $\mu_i(t)$, $f_{\max}$ is the maximum Doppler frequency, and T_A is the sampling interval. A subset of $\mathbf{\Psi}$ is $\psi = (\sigma_0, f_{\max}, T_A)$, and its elements are given by [31]:

$$\sigma_0 = \frac{r_{th}}{\sqrt{2\ln(1+\mathcal{R}_B)}} \quad (17)$$

$$f_{\max} = \frac{\mathcal{N}_{EB}(1+\mathcal{R}_B)}{T_t\sqrt{2\pi\ln(1+\mathcal{R}_B)}} \quad (18)$$

$$T_A \approx \frac{4\sigma_0\left[\exp\left(\frac{r_{th}^2}{2\sigma_0^2}\right)-1\right]}{\sqrt{5}\pi r_{th} f_{\max}} \sqrt{-1+\sqrt{1+10q_s/3}}. \quad (19)$$

The value of $\mathcal{R}_B$ is the ratio of the mean value of error burst lengths to the mean value of error-free burst lengths. The parameter T_t is the total transmission time of the communications system. The quantity q_s is the maximum measurement error of the level-crossing rate (LCR).

When the simulation is run, the deterministic process varies in a way that it crosses the threshold with positive and negative slopes. Second-order statistics of the sampled deterministic process, such as the LCR, average duration of fades (ADF), and average duration of inter-fades (AIDF), can be worked out. When the level of the deterministic process is above that threshold (inter-fading intervals), an error-free burst is generated. On the contrary, when the deterministic level is below the threshold (fading intervals), an error burst is generated. The lengths of the error-free bursts and error bursts is equal to the number of samples counted in inter-fading and fading intervals, respectively. Subsequently, error burst and error-free burst generators are produced as vectors, i.e., $\widetilde{\mathbf{EB}}_{rec}$ and $\widetilde{\mathbf{EFB}}_{rec}$ with length distributions $\tilde{P}_{EB}$ and $\tilde{P}_{EFB}$, respectively. The tilde sign is placed on parameters related to the generative model to distinguish them from those of the reference error sequence.

Mapping [31] is then employed to adjust the generated error and error-free burst lengths. This means that mappers modify $\widetilde{\mathbf{EB}}_{rec}$ and $\widetilde{\mathbf{EFB}}_{rec}$ such that $\tilde{N}_{EB}(m_e) = \hat{N}_{EB}(m_e)$ and $\tilde{N}_{EFB}(m_{\bar{e}}) = \hat{N}_{EFB}(m_{\bar{e}})$ hold, respectively. Here, $\hat{N}_{EB}(m_e)$ is equal to $\lfloor(\tilde{N}_t/N_t)N_{EB}(m_e)\rfloor$ or $\lfloor(\tilde{N}_t/N_t)N_{EB}(m_e)\rfloor + 1$ for different error burst lengths m_e in order to fulfill $\sum_{m_e=m_{B1}}^{m_{B2}} \hat{N}_{EB}(m_e) = \tilde{\mathcal{N}}_{EB} = \lfloor(\tilde{N}_t/N_t)\mathcal{N}_{EB}\rfloor$. Similarly, $\hat{N}_{EFB}(m_{\bar{e}})$ is equal to $\lfloor(\tilde{N}_t/N_t)N_{EFB}(m_{\bar{e}})\rfloor$ or $\lfloor(\tilde{N}_t/N_t)N_{EFB}(m_{\bar{e}})\rfloor + 1$ for different error-free burst lengths $m_{\bar{e}}$ to satisfy $\sum_{m_{\bar{e}}=m_{\bar{B}1}}^{m_{\bar{B}2}} \hat{N}_{EFB}(m_{\bar{e}}) = \tilde{\mathcal{N}}_{EFB} = \lfloor(\tilde{N}_t/N_t)\mathcal{N}_{EFB}\rfloor$. To modify $\widetilde{\mathbf{EB}}_{rec}$, we first find the corresponding values $\ell^1_{m_e}$ and $\ell^2_{m_e}$ in $\widetilde{\mathbf{EB}}_{rec}$ to assure the following conditions [31]:

$$\sum_{l=\ell^1_{m_e}}^{\ell^2_{m_e}-1} \tilde{N}_{EB}(l) < \hat{N}_{EB}(m_e)$$
$$\sum_{l=\ell^1_{m_e}}^{\ell^2_{m_e}} \tilde{N}_{EB}(l) \geq \hat{N}_{EB}(m_e). \quad (20)$$

Then,

$$\sum_{l=\ell^1_{m_e}}^{\ell^2_{m_e}-1} \tilde{N}_{EB}(l) + N_{EB}\left(\ell^2_{m_e}\right) = \hat{N}_{EB}(m_e). \quad (21)$$

The same idea applies to $\widetilde{\mathbf{EFB}}_{rec}$. It is clear that the mappers refit $l(\ell^1_{m_e} \leq l \leq \ell^2_{m_e} - 1)$ samples of the fading process in each interval to m_e, which is the required burst length. After mapping, error sequences can be obtained by combining the consecutively generated error bursts with error-free bursts.

Once all the above parameters are known, an error sequence with any desirable length can be generated. Therefore, the key to generate a new error sequence Z with any required SNR from two reference error sequences X and Y, having different SNRs, i.e., SNR_X and SNR_Y, is to obtain the parameters ψ, $\tilde{P}_{EB}(m_e)$, $\tilde{P}_{EFB}(m_{\bar{e}})$, $\hat{N}_{EB}(m_e)$, and $\hat{N}_{EFB}(m_{\bar{e}})$ for the error sequence Z from similar parameters of the error sequences X and Y. Again, our investigations have demonstrated that these parameters or burst error statistics will linearly increase with the increase or decrease of SNRs in dB. Similar to the derivations in (8)–(12), we can obtain ψ_Z and $\tilde{P}_{EB_Z}$ from

$$\psi_Z = \alpha \cdot \psi_X + \beta \cdot \psi_Y. \quad (22)$$
$$\tilde{P}_{EB_Z} = \alpha \cdot \tilde{P}_{EB_X} + \beta \cdot \tilde{P}_{EB_Y}. \quad (23)$$

respectively, where α and β are given by (11) and (12), respectively.

In order to construct $\widetilde{\mathbf{EB}}_{rec}$ from $\tilde{P}_{EB_Z}$, we have to know the total number of error bursts $\tilde{\mathcal{N}}_{EB}$ for the error sequence Z. The number $\tilde{\mathcal{N}}_{EB_Z}$ is obtained by interpolating between $\tilde{\mathcal{N}}_{EB_X}$ and $\tilde{\mathcal{N}}_{EB_Y}$, given that X and Y have the same length. Multiplying the obtained number with the extracted $\tilde{P}_{EB_Z}$ with some manipulations related to the CDF gives us the required $\widetilde{\mathbf{EB}}_{rec}$ of Z. Similar procedure can be applied to find $\widetilde{\mathbf{EFB}}_{rec}$. In order to apply the mappers, we need to find $\hat{N}_{EB}(m_e)$ corresponding to Z by finding P_{EB_Z} as follows:

$$P_{EB_Z} = \alpha \cdot P_{EB_X} + \beta \cdot P_{EB_Y}. \quad (24)$$

The EBD $P_{EB}(m_e)$ linearly increases with the increase of SNRs in dB for any given error burst length m_e, as clearly indicated in Fig. 2. Now, we have to work out the total numbers of error bursts $\mathcal{N}_{EB_Z}$ for the error sequence Z by interpolating between $\mathcal{N}_{EB_X}$ and $\mathcal{N}_{EB_Y}$ given that X and Y have the same length, and then, we find $\hat{N}_{EB}(m_e)$. Similar methodology can be applied to find $\hat{N}_{EFB}(m_e)$. Consequently, mappers are used according to (20) and (21) to work out the modified $\widetilde{\mathbf{EB}}_{rec}$ and $\widetilde{\mathbf{EFB}}_{rec}$.

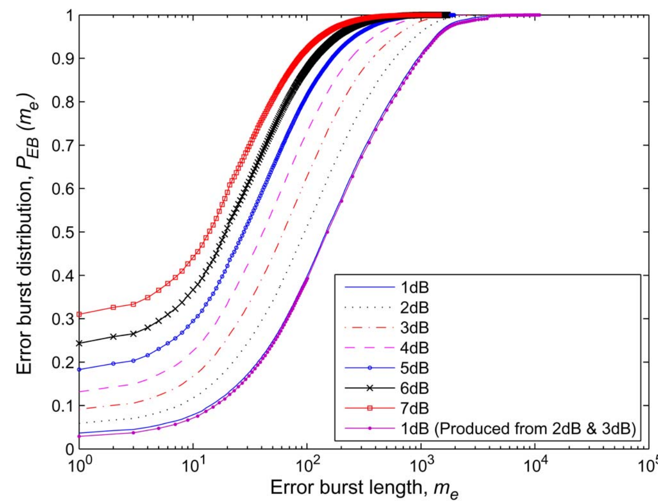

Fig. 2. The EBDs of the descriptive model for several SNRs and reproduced EBD.

Afterwards, we can create error bursts and error-free bursts according to the lengths in the modified $\widetilde{\mathbf{EB}}_{rec}$ and $\widetilde{\mathbf{EFB}}_{rec}$. Generating error-free bursts is simple because the lengths of the modified $\widetilde{\mathbf{EFB}}_{rec}$ can easily be converted to series of zeros, unlike error bursts which contain zeros and ones. Generating error bursts involves retrieving their structures from the error bursts of error sequences X and Y. The retrieved error bursts have the same length m_e as in the newly obtained $\widetilde{\mathbf{EB}}_{rec}$ of Z. Finally, the error bursts and error-free bursts are combined together to construct the new required error sequence Z.

IV. Simulation Results and Discussions

To validate our proposed adaptive generative models, we first need to obtain reference error sequences, which are essential to initialize various parameters for the generative models. We used an uncoded LTE system to obtain the required reference error sequences. The performance criteria are the burst error statistics defined in Section II. A generative model is better if its burst error statistics better match those of the descriptive model, particularly the most important statistics such as the BEPD and BECF.

The uncoded LTE system [38] has a burst interleaver, rate matcher, adaptive modulation and coding (AMC), a viterbi equalizer, and a burst deinterleaver. The utilized propagation channel can be expressed as NAMEx, where x represents the vehicle speed in km/h. NAME here represents the name of the underlying channel, e.g., a rural area (RA) channel, a typical urban (TU) channel, or a pedestrian B (PedB) channel. We used the following channels: RA275, TU3, TU50, PedB5, and PedB10. The received data has a length of 12×10^6, and the transmission rate is $F_s = 3450$ kb/s. Reference error sequences were produced at SNRs of 1 dB, . . ., 7 dB.

By comparing the transmitted error sequence with the received one, we work out the bit error sequences. We use the three discussed generative models, namely, ASFM, ABWHMM, and ADPBGM, in order to generate new error sequences of length 15×10^6 bits based on the obtained error sequences from the LTE system. In this paper, we show only the results of the TU50 channel having SNRs of 2 dB, 3 dB, 4 dB, and 5 dB.

For the ASFM, the fitting of $P(0^{m_0}|1)$ is achieved by using five exponentials, and therefore, $N = 6$ holds. In our experiments, no better performance can be accomplished for SFMs with more than six states. After we fit (3) with $P(0^{m_0}|1)$ of SNRs $= 2$ dB, 3 dB, and 5 dB, we can obtain the transition matrices from which we can generate new error sequences. Afterwards, we apply (10)–(12) to calculate the adaptive $P_Z(0^{m_0}|1)$. Once we know the adaptive $P_Z(0^{m_0}|1)$, (1) and (3) can be applied to generate new error sequences Z.

For the ABWHMM, we extract the error bursts from error sequences with SNRs $= 3$ dB and 5 dB. Then, we divide each error burst into blocks with $L = 20$ bits and obtain the $\mathbf{NEL}_h$ vectors. We apply (14) afterwards to obtain the $\mathbf{NEL}_{hZ}$ vectors. A Baum-Welch training process was then applied to $\mathbf{NEL}_{hZ}$ after classifying it into a satisfactory number of states. The number of classes $\mathbb{N}$ is 7 in our example, and the number of substates is considerably large. Finally, the generated error bursts are concatenated with the generated error-free bursts in order to produce the full required error sequence.

In order to proceed with the ADPBGM, we need to find the vector $\mathbf{\Psi}$. The value of q_s was chosen as 0.01. For the error sequences with SNRs $= 2$ dB, 3 dB, and 5 dB, $\mathcal{N}_{EB} = 428418$, 69706, and 122474 and $\mathcal{R}_B = 8.43$, 5.24, and 2.09, respectively. Consequently, $\mathbf{\Psi} = (9, 10, 0.09, 0.0425, 34.9\ \text{kHz}, 8.33\ \mu\text{s})$ for SNR $= 2$ dB, $\mathbf{\Psi} = (9, 10, 0.09, 0.0470, 36.8\ \text{kHz}, 5.43\ \mu\text{s})$ for SNR $= 3$ dB, and $\mathbf{\Psi} = (9, 10, 0.09, 0.0599, 40.9\ \text{kHz}, 4.97\ \mu\text{s})$ for SNR $= 5$ dB. For the new required error sequence Z, the vector $\mathbf{\Psi}_Z$ can be obtained by (22). Then, we find $\tilde{N}_{EB}(m_e)$ and the modified $\hat{N}_{EB}(m_e)$ for the error sequence Z with the aid of (23) and (24). Similarly, $\tilde{N}_{EFB}(m_e)$ and the modified $\hat{N}_{EFB}(m_e)$ can be found.

Eventually, the error bursts and error-free bursts are combined to construct entailed error sequences Z. The bit structure in the new error bursts is retrieved from the two reference error sequences X and Y based on the error burst lengths.

In the following, we focus on simulations where SNR$_Z$ is between SNR$_X$ and SNR$_Y$ due to limited space. However, other SNR values are applicable to our adaptive models, as shown in Figs. 1 and 2. Here, we produce an error sequence Z with SNR $= 4$ dB from reference error sequences X with SNR $=$ 3 dB and Y with SNR $= 5$ dB (first scenario, Figs. 3–7). We also produce an error sequence Z with SNR $= 4$ dB from error sequences X with SNR $= 2$ dB and Y with SNR $= 5$ dB (second scenario, Figs. 8–11). This means that $\alpha = \beta = 0.5$ for the first scenario and $\alpha = 1/3$ and $\beta = 2/3$ for the second scenario. The second scenario investigates the impact of further distancing the SNRs of error sequences X and Y from the SNR of error sequences Z. We compare the burst error statistics of error sequences Z, obtained from both scenarios, with those statistics obtained from the reference error sequence of the LTE simulator having SNR $= 4$ dB. In terms of parametrization, the value of η can be found from Fig. 1 when the curve is tending to turn, and it was chosen to be 20.

Figs. 3–11 illustrate various burst error statistics of the descriptive model and adaptive generative models such as the ECDs (Figs. 3 and 11), BEPDs (Figs. 4 and 8), BECFs (Figs. 5 and 9), EBDs (Figs. 6 and 10), EFRDs (Fig. 1), and GDs (Fig. 7). Figs. 3–7 omit the comparison between the DPBGM and the ADPBGM since the DPBGM gives approximate results to the descriptive one [31]. In general, the ADPBGM shows

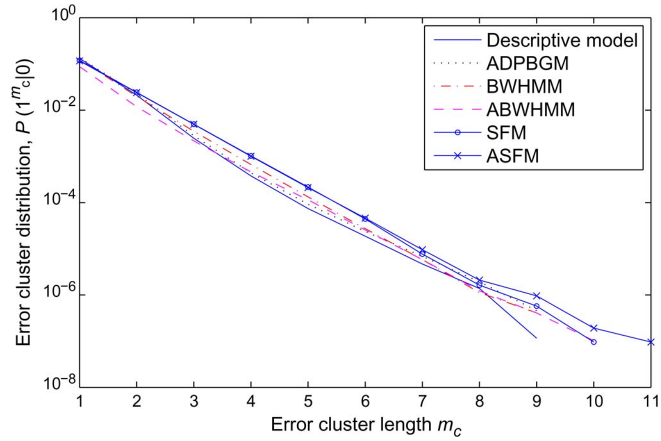

Fig. 3. The ECDs of the descriptive model, generative models, and three adaptive generative models (SNR $= 4$ dB obtained from 3 dB and 5 dB).

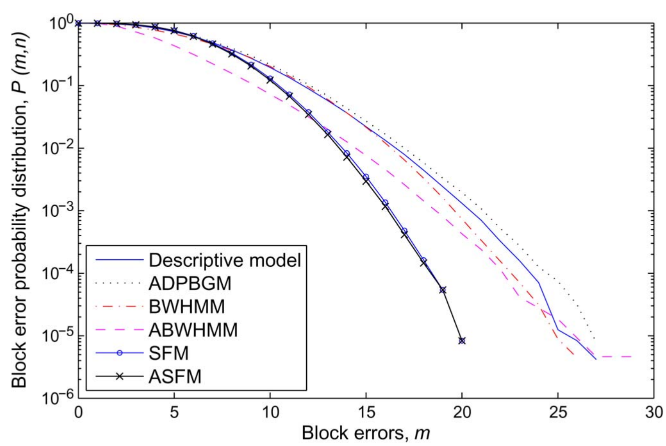

Fig. 4. The BEPDs of the descriptive model, generative models, and three adaptive generative models (SNR $= 4$ dB obtained from 3 dB and 5 dB, $n = 50$).

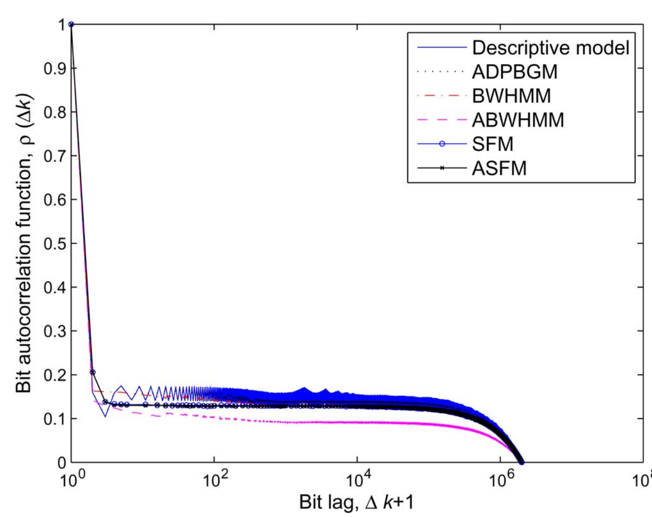

Fig. 5. The BECFs of the descriptive model, generative models, and three adaptive generative models (SNR $= 4$ dB obtained from 3 dB and 5 dB).

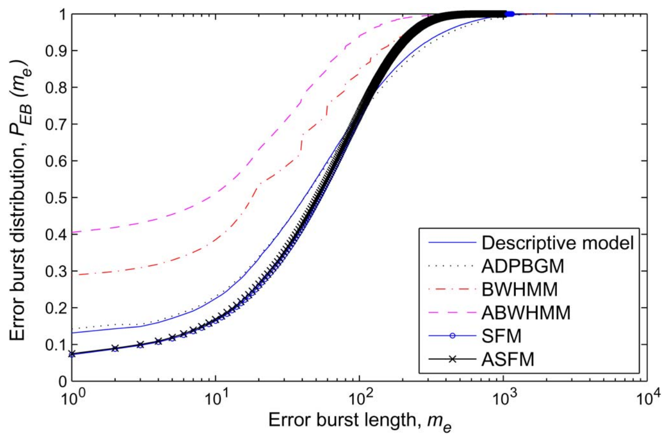

Fig. 6. The EBDs of the descriptive model, generative models, and three adaptive generative models (SNR = 4 dB obtained from 3 dB and 5 dB).

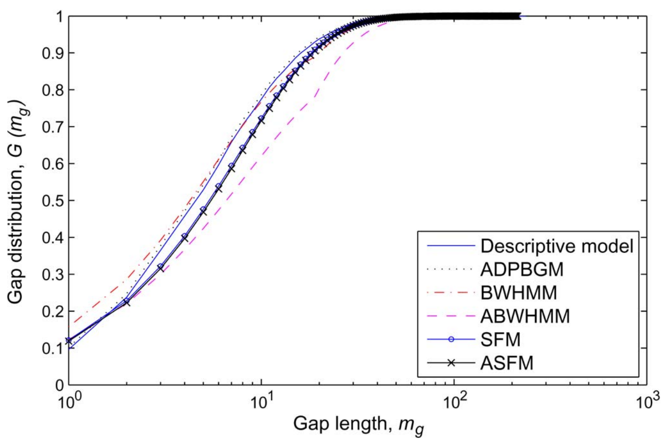

Fig. 7. The GDs of the descriptive model, generative models, and three adaptive generative models (SNR = 4 dB obtained from 3 dB and 5 dB).

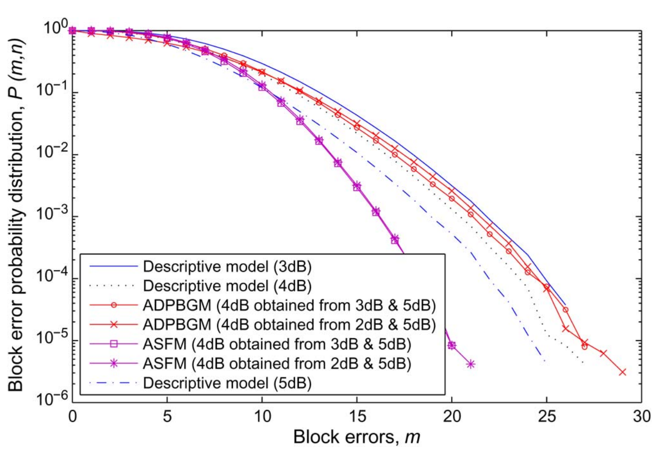

Fig. 8. The BEPDs of the descriptive model, ASFM, and ADPBGM ($n = 50$).

the best fit to the descriptive model. This is clear for all the burst error statistics, except a small mismatch at the end of the curve of the ECD (see Fig. 3) and the BEPD (see Fig. 4). The second best generative model is the ASFM, although its burst error statistics considerably mismatch those of the ADPBGM. However, the ASFM and the SFM fit each other. The ABWHMM results are slightly worse than those obtained using the normal BWHMM procedure.

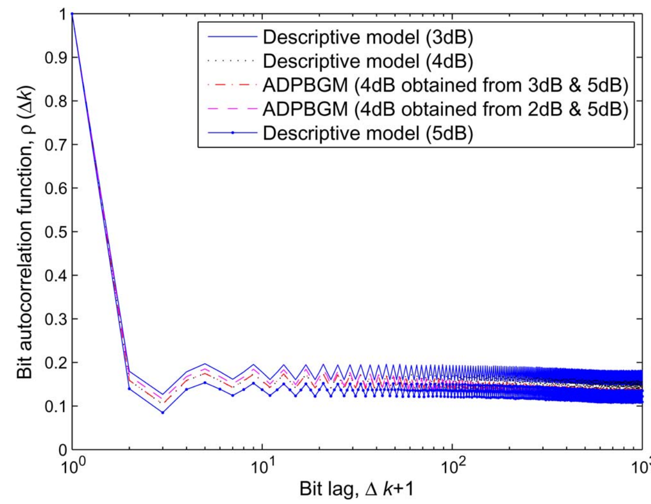

Fig. 9. The BECFs of the descriptive model and ADPBGM.

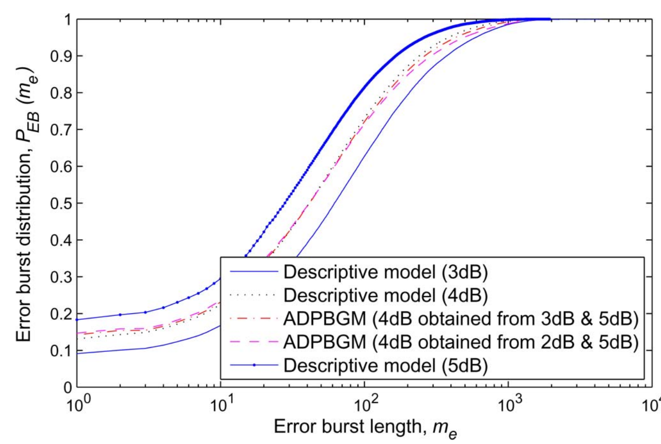

Fig. 10. The EBDs of the descriptive model and ADPBGM ($n = 50$).

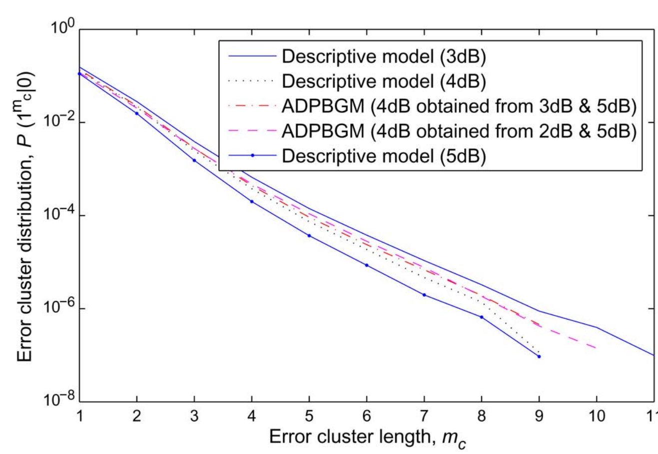

Fig. 11. The ECDs of the descriptive model and ADPBGM.

In Figs. 8–11, we omit the results of the ABWHMM because its burst error statistics do not match those of the BWHMM. Fig. 8 shows the BEPDs of the descriptive model for SNRs $= 3$ dB, 4 dB, and 5 dB, as well as the BEPDs of the ADPBGM and the ASFM for SNR $= 4$ dB obtained from two scenarios, i.e., from SNRs $= 3$ dB and 5 dB and SNRs $=$ 2 dB and 5 dB. It is found that distancing the SNRs that are required to produce the new error sequence can deteriorate the

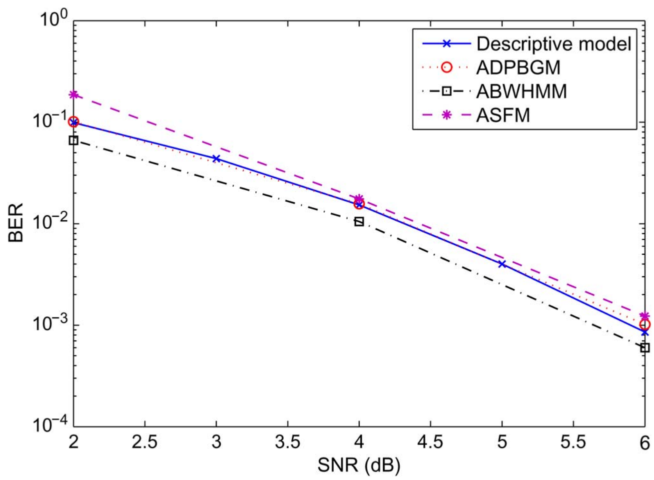

Fig. 12. The coded BER of the descriptive model and three adaptive generative models.

performance of the ADPBGM. On the other hand, the ASFM is not affected by distancing the reference SNRs, although the general performance of the ASFM is not satisfactory (far from the descriptive model). In Figs. 9–11, we illustrate the BECFs, EBDs, and ECDs of the descriptive model for SNRs = 3 dB, 4 dB, and 5 dB, as well as those of the ADPBGM for SNR = 4 dB obtained from two scenarios, respectively, while neglecting the results for ASFM and ABWHMM. It is clear that the ADPBGM is slightly affected by changing the values of α and β. Fig. 12 shows the BER performance of the coded LTE system using the original error sequence (descriptive model) and newly generated error sequences using three adaptive generative models. Note that the new error sequences Z of the three generative models were obtained from two neighboring error sequences X and Y with SNRs distancing 1 dB from the SNR of error sequences Z, i.e., $\alpha = \beta = 1/2$. It is apparent that the ADPBGM outperforms the ASFM and the ABWHMM in terms of fitting the coded BER performance.

Regarding the simulation time, obtaining a reference error sequence with a length of 12 million bits can take more than 10 hours. Generating an error sequence with the same length using generative models can take just a few minutes or seconds [31]. However, it takes adaptive generative models a few seconds to generate many new error sequences. Therefore, adaptive generative models are very efficient in terms of saving the simulation time as we can simply use two reference error sequences to produce many new error sequences.

V. CONCLUSION

Adaptive generative models are highly desirable because they can generate new error sequences with any channel conditions (or SNRs) utilizing limited available reference error sequences. Compared to descriptive models and traditional generative models, adaptive generative models can significantly reduce the computational time when we need a huge number of error sequences for the purpose of evaluating the performance of a digital communication system. In this paper, we have proposed three adaptive generative models, i.e., ADPBGM, ASFM, and ABWHMM. To validate our proposed adaptive algorithms, we have used uncoded LTE system to obtain a few reference error sequences at various SNRs. It has been illustrated through simulations that the ADPBGM can well fit the descriptive model and the DPBGM in terms of both burst error statistics and fitting the BER performance of the coded LTE system. The ASFM and the ABWHMM give poor burst error statistics compared to those of the descriptive model. However, the ASFM is superior to the ABWHMM regarding most of the burst error statistics. It has also been found that the burst error statistics of the ASFM match those of the SFM, while the burst error statistics of the ABWHMM do not match those of the BWHMM.

REFERENCES

[1] J. G. Proakis, Ed., *Digital Communications*, 4th ed. New York, NY, USA: McGraw-Hill, 2001.

[2] H.-H. Hung and L.-J. Chen, "An analytical study of wireless error models for bluetooth networks," in *Proc. AINAW*, Okinawa, Japan, Mar. 2008, pp. 1317–1322.

[3] P. M. Crespo, R. M. Pelz, and J. Cosmas, "Channel error profiles for DECT," *Proc. Inst. Elect. Eng.—Commun.*, vol. 141, no. 6, pp. 413–420, Dec. 1994.

[4] L. N. Kanal and A. R. K. Sastry, "Models for channels with memory and their applications to error control," *Proc. IEEE*, vol. 66, no. 7, pp. 724–744, Jul. 1978.

[5] M. Zorzi, R. R. Rao, and L. B. Milstein, "ARQ error control for fading mobile radio channels," *IEEE Trans. Veh. Technol.*, vol. 46, no. 2, pp. 445–455, May 1997.

[6] M. Zorzi and R. R. Rao, "Perspectives on the impact of error statistics on protocols for wireless networks," *IEEE Pers. Commun.*, vol. 6, no. 10, pp. 32–40, Oct. 1999.

[7] G. Mazzini, "Queue system with smart ARQ on Markov channel for energy efficiency," in *Proc. IWCMC*, Jun. 2005, pp. 546–551.

[8] L. Badia, N. Baldo, M. Levorato, and M. Zorzi, "A Markov framework for error control techniques based on selective retransmission in video transmission over wireless channels," *IEEE J. Sel. Areas Commun.*, vol. 28, no. 3, pp. 488–500, Apr. 2010.

[9] L. Badia, "On the effect of feedback errors in Markov models for SR ARQ packet delays," in *Proc. IEEE GLOBECOM*, Honolulu, HI, USA, Dec. 2009, pp. 3745–3750.

[10] C. Jiao, L. Schwiebert, and B. Xu, "On modeling the packet error statistics in bursty channels," in *Proc. IEEE LCN*, Tampa, FL, USA, Nov. 2002, pp. 534–541.

[11] A. Willig, "A new class of packet- and bit-level models for wireless channels," in *Proc. IEEE PIMRC*, Lisbon, Portugal, Sep. 2002, pp. 2434–2440.

[12] E. N. Gilbert, "Capacity of a burst-noise channel," *Bell Syst. Tech. J.*, vol. 39, no. 5, pp. 1253–1265, Sep. 1960.

[13] E. O. Elliot, "Estimates of error rates for codes on burst-noise channels," *Bell Syst. Tech. J.*, vol. 42, no. 5, pp. 1977–1997, Sep. 1963.

[14] B. D. Fritchman, "A binary channel characterization using partitioned Markov chains," *IEEE Trans. Inf. Theory*, vol. IT-13, no. 2, pp. 221–227, Apr. 1967.

[15] H. S. Wang and N. Moayeri, "Finite-state Markov channel—A useful model for radio communication channels," *IEEE Trans. Veh. Technol.*, vol. 44, no. 1, pp. 163–171, Feb. 1995.

[16] F. De Rango, F. Veltri, and S. Marano, "Channel modeling approach based on the concept of degradation Level discrete-time Markov chain: UWB system case study," *IEEE Trans. Wireless Commun.*, vol. 10, no. 4, pp. 1098–1107, Apr. 2011.

[17] K. Fukawa, H. Suzuki, and Y. Tateishi, "Packet error rate analysis using Markov models of signal-to-interference ratio for mobile packet systems," *IEEE Trans. Veh. Techol.*, vol. 61, no. 6, pp. 2517–2530, Jul. 2012.

[18] F. Swarts and H. C. Ferreira, "Markov characterization of digital fading mobile VHF channels," *IEEE Trans. Veh. Technol.*, vol. 43, no. 4, pp. 977–985, Nov. 1994.

[19] A. Semmar, M. Lecours, J. Y. Chouinard, and J. Ahern, "Characterization of error sequences in UHF digital mobile radio channels," *IEEE Trans. Veh. Technol.*, vol. 40, no. 4, pp. 769–776, Nov. 1991.

[20] W. Turin, *Digital Transmission Systems: Performance Analysis and Modeling*. New York, NY, USA: McGraw-Hill, 1999.

[21] J. Garcia-Frias and P. M. Crespo, "Hidden Markov models for burst error characterization in indoor radio channels," *IEEE Trans. Veh. Technol.*, vol. 46, no. 6, pp. 1006–1020, Nov. 1997.

[22] O. S. Salih, C.-X. Wang, and D. I. Laurenson, "Double embedded processes based hidden Markov models for binary digital wireless channels," in *Proc. IEEE ISWCS*, Reykjavik, Iceland, Oct. 2008, pp. 219–223.

[23] M. U. Ilyas and H. Radha, "Modeling, estimating and predicting the packet-level bit error rate process in IEEE 802.15.4 LR-WPANs using hidden Markov models," in *Proc. CISS*, Baltimore, MD, USA, Mar. 18–20, 2009, pp. 241–246.

[24] L. R. Rabiner, "A tutorial on hidden Markov models and selected applications in speech recognition," *Proc. IEEE*, vol. 77, no. 2, pp. 257–286, Feb. 1989.

[25] W. Zhu and J. Garcia-Frias, "Stochastic context-free grammars and hidden Markov models for modeling of bursty channels," *IEEE Trans. Veh. Technol.*, vol. 53, no. 3, pp. 666–676, May 2004.

[26] E. Costamagna, L. Favalli, and P. Gamba, "Multipath channel modeling with chaotic attractors," *Proc. IEEE*, vol. 90, no. 5, pp. 842–859, May 2002.

[27] E. Costamagna, L. Favalli, P. Gamba, and P. Savazzi, "Block-error probabilities for mobile radio channels derived from chaos equations," *IEEE Commun. Lett.*, vol. 3, no. 3, pp. 66–68, Mar. 1999.

[28] E. Costamagna, L. Favalli, P. Savazzi, and F. Tarantola, "Long sequences of error gaps derived from chaotic generators optimized for short ones in mobile radio channels," in *Proc. IEEE VTC-Fall*, Los Angeles, CA, USA, Sep. 2004, pp. 4250–4254.

[29] A. Köpke, A. Willig, and H. Karl, "Chaotic maps as parsimonious bit error models of wireless channels," in *Proc. IEEE INFOCOM*, San Francisco, CA, USA, Mar. 30–Apr. 3, 2003, pp. 513–523.

[30] C. X. Wang and M. Pätzold, "A generative deterministic model for digital mobile fading channels," *IEEE Commun. Lett.*, vol. 8, no. 4, pp. 223–225, Apr. 2004.

[31] C.-X. Wang and W. Xu, "A new class of generative models for burst-error characterization in digital wireless channels," *IEEE Trans. Commun.*, vol. 55, no. 3, pp. 453–462, Mar. 2007.

[32] Y. He, O. Salih, C.-X. Wang, and D. Yuan, "Deterministic process based generative models for characterizing packet-level bursty error sequences," *Wireless Commun. Mobile Comput.*, 2013, DOI:10.1002/wcm.2356, to be published.

[33] S. Tsai, "Markov characterization of the HF channel," *IEEE Trans. Commun. Technol.*, vol. COM-17, no. 1, pp. 24–32, Feb. 1969.

[34] W. C. Jakes, Ed., *Microwave Mobile Communications*, 2nd ed. Piscataway, NJ, USA: IEEE, 1994.

[35] C.-X. Wang, M. Pätzold, and D. Yuan, "Accurate and efficient simulation of multiple uncorrelated Rayleigh fading waveforms," *IEEE Trans. Wireless Commun.*, vol. 6, no. 3, pp. 833–839, Mar. 2007.

[36] C.-X. Wang, D. Yuan, H.-H. Chen, and W. Xu, "An improved deterministic SoS channel simulator for efficient simulation of multiple uncorrelated Rayleigh fading channels," *IEEE Trans. Wireless Commun.*, vol. 7, no. 9, pp. 3307–3311, Sep. 2008.

[37] M. Pätzold, C.-X. Wang, and B. O. Hogstad, "Two new sum-of-sinusoids-based methods for the efficient generation of multiple uncorrelated Rayleigh fading waveforms," *IEEE Trans. Wireless Commun.*, vol. 8, no. 6, pp. 3122–3131, Jun. 2009.

[38] C. Mehlführer, M. Wrulich, J. C. Ikuno, D. Bosanska, and M. Rupp, "Simulating the long term evolution physical layer," in *Proc. EUSIPCO*, Glasgow, U.K., Aug. 2009, pp. 1471–1478.

Omar S. Salih (S'07–M'14) received the Ph.D. degree in electrical and electronic engineering jointly from the Institute of Sensors, Signals, and Systems, Heriot-Watt University, Edinburgh, U.K., and the Institute of Digital Communications, University of Edinburgh, Edinburgh.

He is currently an Assistant Lecturer with the Department of Aviation, Aerospace, Electrical and Electronic Engineering, Coventry University, Coventry, U.K. His main research interests are in digital channel modeling, propagation and channel characterization, 4G and 5G cellular systems, DSP applications to wireless systems, resource allocation and load balancing, and adaptive antennas for wireless systems.

Cheng-Xiang Wang (S'01–M'05–SM'08) received the B.Sc. and M.Eng. degrees in communication and information systems from Shandong University, Jinan, China, in 1997 and 2000, respectively, and the Ph.D. degree in wireless communications from Aalborg University, Aalborg, Denmark, in 2004.

Since 2005, he has been with Heriot-Watt University, Edinburgh, U.K., where he became a Professor in 2011. He is also an Honorary Fellow with the University of Edinburgh and a Chair/Guest Professor with Shandong University and Southeast University, Nanjing, China. He was a Research Fellow with the University of Agder, Grimstad, Norway, from 2001 to 2005; a Visiting Researcher with Siemens AG-Mobile Phones, Munich, Germany, in 2004; and a Research Assistant with Technical University of Hamburg-Harburg, Hamburg, Germany, from 2000 to 2001. His current research interests include wireless channel modeling and simulation, massive MIMO, green communications, cognitive radio networks, vehicular communication networks, and 5G wireless communications. He has edited one book and published one book chapter and over 200 papers in refereed journals and conference proceedings.

Prof. Wang served or is currently serving as an Editor of eight international journals, including the IEEE TRANSACTIONS ON VEHICULAR TECHNOLOGY (2011-) and the IEEE TRANSACTIONS ON WIRELESS COMMUNICATIONS (2007–2009). He was the leading Guest Editor of the IEEE JOURNAL ON SELECTED AREAS IN COMMUNICATIONS, Special Issue on Vehicular Communications and Networks. He served or is serving as a TPC member, a TPC Chair, and a General Chair for over 70 international conferences. He received the Best Paper Awards from IEEE Globecom 2010, IEEE ICCT 2011, ITST 2012, and IEEE VTC 2013-Fall. He is a Fellow of the IET, a Fellow of the HEA, and a member of EPSRC Peer Review College.

Bo Ai (M'00–SM'10) received the M.S. and Ph.D. degrees from Xidian University, Xi'an, China, in 2002 and 2004, respectively. He graduated in 2007 with great honors of Excellent Postdoctoral Research Fellow from Tsinghua University.

He is currently a Professor and an Advisor of Ph.D. candidates with Beijing Jiaotong University. He is also a Deputy Director of the State Key Laboratory of Rail Traffic Control and Safety. He has authored/co-authored 6 books, 140 scientific research papers, and 26 invention patents in his research area. His current interests are the research and applications of OFDM techniques, HPA linearization techniques, radio propagation and channel modeling, GSM for railway systems, and LTE for railway systems. He has received many awards including the Qiushi Outstanding Youth Award from the Hong Kong Qiushi Foundation, the New Century Talents Award from the Chinese Ministry of Education, the Zhan Tianyou Railway Science and Technology Award from the Chinese Ministry of Railways, and the Science and Technology New Star Award from the Beijing Municipal Science and Technology Commission. He is an Associate Editor of IEEE TRANSACTIONS ON CONSUMER ELECTRONICS and an Editorial Committee Member of the journal *Wireless Personal Communications*. He is the Co-Chair or the Session/Track chair of many international conferences such as the 9th International Heavy Haul Conference in 2009, IEEE ICIRT 2011, HSRCom2011, IEEE ISCE 2012, ICWMMN 2013, IEEE Green HetNet 2013, and IEEE 78th VTC 2014. He is an IET Fellow.

Raed Mesleh (S'00–M'08–SM'13) received the Ph.D. degree in electrical engineering from Jacobs University Bremen, Bremen, Germany, and has several years of post-doctoral wireless communication and optical wireless communication research experience in Germany. In October 2010, he joined the University of Tabuk, Tabuk, Saudi Arabia, where he is now an Assistant Professor in the Electrical Engineering Department and the Director of research excellence and intellectual properties units. He invented spatial modulation, trellis coded spatial modulation and the use of OFDM for visible light communication. His main research interests are in spatial modulation, MIMO cooperative wireless communication techniques and optical wireless communication. His publications have received more than 1400 citations since 2007. He has published more than 70 journal and conference papers and holds 7 patents. In 2012, he received the IEEE COMMUNICATION LETTER Exemplary Reviewer Certificate.